Contribution from the Department of Chemistry,
The University of Calgary, Calgary T2N 1N4, Alberta, Canada

Lewis Base Properties of $1\lambda^5$-Phospha-3,5-dithia-2,4,6-triazines: Crystal and Molecular Structures of $Ph_2PS_2N_3Me^+CF_3SO_3^-$ and *trans*-$(Ph_2PS_2N_3)_2SnCl_4$ and the Electronic Structure of $H_2PS_2N_3H^+$

Tristram Chivers,* Stephen W. Liblong, John F. Richardson, and Tom Ziegler

Received September 22, 1987

The behavior of $Ph_2PS_2N_3$ toward Lewis and Brønsted acids has been investigated, and the following adducts have been isolated: $Ph_2PS_2N_3H^+BF_4^-$, $Ph_2PS_2N_3H^+CF_3SO_3^-$, $Ph_2PS_2N_3Me^+CF_3SO_3^-$, $Ph_2PS_2N_3{\cdot}BCl_3$, and $(Ph_2PS_2N_3)_nSnCl_4$ (n = 1, 2). The progress of the reaction of $Ph_2PS_2N_3$ with tetrafluoroboric acid was followed by ^{31}P NMR and UV-visible spectroscopies. The adducts exhibit strong visible absorption bands at 410-430 nm. The crystal and molecular structures of $Ph_2PS_2N_3Me^+CF_3SO_3^-$ (**5**) and *trans*-$(Ph_2PS_2N_3)_2SnCl_4$ (**6**) have been determined by X-ray crystallography. The crystals of **5** are monoclinic and belong to the space group $P2_1/a$, with a = 11.857 (3) Å, b = 13.708 (2) Å, c = 12.417 (3) Å, β = 111.410 (11)°, V = 1879.0 (7) Å^3, and Z = 4. The final R and R_w values were 0.050 and 0.054, respectively. The crystals of **6** are monoclinic and belong to the space group $P2_1/n$, with a = 9.238 (1) Å, b = 10.586 (1) Å, c = 21.752 (4) Å, β = 95.320 (8)°, V = 2118.1 (5) Å^3, and Z = 2. The final R and R_w values were 0.037 and 0.042, respectively. In both adducts, coordination occurs at a nitrogen atom adjacent to the phosphorus atom of the PS_2N_3 ring and the coordinated nitrogen atom is lifted 0.78 and 0.71 Å for **5** and **6**, respectively, out of the plane formed by the remaining five atoms (SNSNP) of the heterocyclic ring. The P-N bond distances of 1.65-1.67 Å are slightly longer in the adducts compared to those of the parent ring system (d(P-N) = 1.62 Å), but coordination to nitrogen does not cause a notable difference in the lengths of the two P-N bonds in either **5** or **6**. There are pronounced inequalities in the S-N bond lengths of the NSNSN unit in the adducts. The S-N bond lengths involving the coordinated nitrogen are 1.71 Å, the adjacent S-N bond distances are 1.63-1.64 Å, and the other two S-N bonds have values in the range 1.55-1.56 Å. The geometry around the tin atom in **6** is approximately octahedral with the two heterocyclic rings occupying trans positions. Ab initio Hartree-Fock-Slater SCF calculations of the electronic and electrostatic components of the protonation energies for the model protonated species $H_2PS_2N_3H^+$ show that the preference for protonation at the nitrogen atom adjacent to phosphorus can be attributed entirely to the electrostatic energy contribution. The conformational changes and hypsochromic shift that occur upon adduct formation are discussed in the context of the calculated electronic structures of the model system $H_2PS_2N_3$ by using the experimental geometries for $Ph_2PS_2N_3$ and its methylated derivative.

Introduction

Recently we reported the preparation and structural characterization of the six-membered ring **1** (R = Ph).[1] This heterocycle

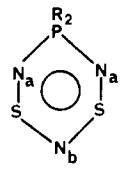

1

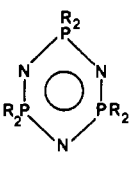

2

is a hybrid of the cyclotriphosphazenes **2** and the cyclotrithiazene anion $S_3N_3^-$ (**3**).[2] Reactivity studies of **1** have so far been restricted to reactions that occur at the sulfur centers, e.g. cycloaddition with olefins[1] and oxidative addition with halogens.[3] The regiospecifity of these reactions can be understood from a consideration of the composition of the frontier orbitals of **1**; both the HOMO and LUMO have π^* characteristics and are based primarily on the sulfur atoms.[1]

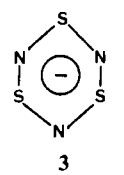

3

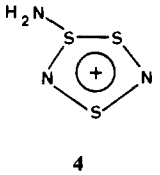

4

Cyclophosphazenes can behave as either Lewis or Brønsted bases forming a variety of adducts with Lewis acids, including the proton, via coordination at an endocyclic nitrogen atom.[4] The limited structural information available for such adducts reveals lengthened skeletal bonds to the protonated nitrogen atoms.[5,6] The interaction of $S_3N_3^-$ with protonic acids, e.g. HBF_4[7a] or other electrophiles[7b], results in a more drastic structural reorganization to give ring-contracted products **4**.[7] The instability of the hypothetical ring system S_3N_3H has been attributed to the ready polarizability of the π-system of **3** in which the degenerate π^*-levels are fully occupied.[7]

The heterocycle **1** is an eight-π-electron system[1,2] and thus may be regarded as intermediate between the electron-precise six-π-electron ring (**2**) and the electron-rich 10-π-electron-system (**3**) in terms of the occupancy of the π-electron manifold. It was of interest, therefore, to determine the effect of the interaction of this hybrid ring system with Lewis and Brønsted acids in order to establish both the site of attack (N_a or N_b) and the structural changes that accompany adduct formation. The possibility of promoting ring-opening and/or polymerization reactions of cyclophosphathiazenes by using Lewis acid catalysts was an additional objective of this investigation.

In the initial phase of this study the protonation of **1** (R = Ph) with HBF_4 was monitored by ^{31}P NMR and UV-visible spectroscopies in order to assess the extent of adduct formation. Subsequently, crystalline adducts were isolated and characterized in the reactions of **1** (R = Ph) with BCl_3, HBF_4, $CH_3SO_3CF_3$, HSO_3CF_3, and $SnCl_4$ and the structures of $Ph_2PS_2N_3Me^+SO_3CF_3^-$ and $(Ph_2PS_2N_3)_2SnCl_4$ were determined by X-ray crystallography. Ab initio Hartree-Fock-Slater (HFS) SCF calculations were carried out on the model system $H_2PS_2N_3H^+$ in order to (a) determine the reason(s) for preferential protonation at the nitrogen adjacent to phosphorus, (b) compare the electronic structure of

(1) Burford, N.; Chivers, T.; Cordes, A. W.; Laidlaw, W. G.; Noble, M.; Oakley, R. T.; Swepston, P. N. *J. Am. Chem. Soc.* **1982**, *104*, 1282.
(2) Bojes, J.; Chivers, T.; Laidlaw, W. G.; Trsic, M. *J. Am. Chem. Soc.* **1979**, *101*, 4517.
(3) Burford, N.; Chivers, T.; Oakley, R. T.; Oswald, T. *Can. J. Chem.* **1984**, *62*, 712.
(4) Heal, H. G. *The Inorganic Heterocyclic Chemistry of Sulfur, Nitrogen and Phosphorus*; Academic: London 1980; p 234.
(5) Trotter, J.; Whitlow, S. H. *J. Chem. Soc. A* **1970**, 460.
(6) Calhoun, H. P.; Oakley, R. T.; Paddock, N. L.; Trotter, J. *Can. J. Chem.* **1975**, *53*, 2413.
(7) (a) Marcellus, C. G.; Oakley, R. T.; Cordes, A. W.; Pennington, W. T. *Can. J. Chem.* **1984**, *62*, 1822. (b) Bojes, J.; Chivers, T. *Inorg. Chem.* **1978**, *17*, 318.
(8) Chivers, T. *Acc. Chem. Res.* **1984**, *17*, 166.
(9) Burford, N.; Chivers, T.; Hojo, M.; Laidlaw, W. G.; Richardson, J. F.; Trsic, M. *Inorg. Chem.* **1985**, *24*, 709.

0020-1669/88/1327-0860$01.50/0

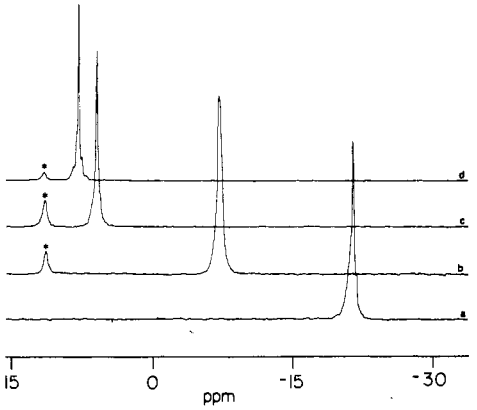

Figure 1. ^{31}P NMR spectra for the reaction of $HBF_4 \cdot Et_2O$ with $Ph_2PS_2N_3$ recorded at molar ratios of 0:1 (a), 0.5:1 (b), 1:1 (c), and 1.5:1 (d). The peak marked with an asterisk is an unidentified impurity.

the protonated species with that of the parent ring system **1** (R = H) in the context of the observed molecular structures, and (c) provide an explanation for the pronounced hypsochromic shift in the visible absorption band of **1** upon adduct formation.

Experimental Section

Reagents and General Procedures. All solvents were dried and distilled before use: carbon tetrachloride and methylene dichloride (P_2O_5), hexanes, pentane, and diethyl ether (Na), and acetonitrile (CaH_2 and P_2O_5). All reactions and the manipulation of moisture-sensitive products were carried out under an atmosphere of nitrogen (99.99% purity) passed through Ridox, P_2O_5, and silica gel. Chemical analyses were performed by the Analytical Services of the Department of Chemistry, University of Calgary, and by MHW Laboratories, Phoenix, AZ.

$Ph_2PS_2N_3$ was prepared according to the literature method.[1] Other chemicals were obtained from Aldrich Chemical Co. and used as received: BCl_3 (1.0 M solution in hexanes), $SnCl_4$ (1.0 M solution in CH_2Cl_2), CF_3SO_3H, $CF_3SO_3CH_3$, and $HBF_4 \cdot Et_2O$.

Instrumentation. Infrared spectra were recorded as Nujol mulls (KBr windows) or KBr pellets on a Nicolet 5DX FT-IR spectrometer. UV–visible spectra were obtained by using a Cary 219 spectrophotometer. NMR spectra were recorded on a Varian XL-200 instrument. ^1H and ^{13}C chemical shifts are referenced to $CHCl_3$ and are reported in ppm downfield from Me_4Si. ^{31}P chemical shifts are referenced to external 85% H_3PO_4.

Spectroscopic Investigation of the Reaction of $Ph_2PS_2N_3$ with HBF_4. The course of this reaction was monitored by ^{31}P NMR spectroscopy using the following procedure. A known weight of $Ph_2PS_2N_3$ was introduced into a septum-sealed 10-mm NMR tube, and a known volume of $CDCl_3$ was added by syringe. This solution was titrated against a solution of $HBF_4 \cdot Et_2O$ in $CDCl_3$ of known concentration by using a calibrated syringe for the addition of the acid, and ^{31}P NMR spectra were recorded for molar HBF_4:$Ph_2PS_2N_3$ ratios of 0:1, 0.5:1, 1:1 and 1.5:1 (see Figure 1). The same reaction was followed by UV–visible spectroscopy using a spectrophotometric cell that was fitted with a rubber septum. A solution of $HBF_4 \cdot Et_2O$ in CH_2Cl_2 of known concentration was added by syringe to a standard solution of $Ph_2PS_2N_3$ in CH_2Cl_2, and spectra were recorded for the same molar HBF_4:$Ph_2PS_2N_3$ ratios as those used in the NMR experiment. The UV–visible spectra are illustrated in Figure 2.

Preparation of $Ph_2PS_2N_3H^+BF_4^-$. An excess of $HBF_4 \cdot Et_2O$ (0.73 g, 4.5 mmol) was added by syringe to a stirred solution of $Ph_2PS_2N_3$ (0.77 g, 8.6 mmol) in 50 mL of diethyl ether. The addition of the tetrafluoroboric acid resulted in an immediate decolorization of the purple solution and the production of a yellow precipitate of $Ph_2PS_2N_3H^+BF_4^-$ (0.95 g, 2.5 mmol), mp 104 °C dec. Anal. Calcd for $C_{12}H_{11}BF_4N_3PS_2$: C, 38.02; H, 2.92; N, 11.08; S, 16.91. Found: C, 37.60; H, 3.30; N, 10.87; S, 15.68. IR (cm^{-1}): 3094 m, 1441 s, 1172 m, 1124 vs, 1111 vs, 1068 s, 1033 m, 1016 m, 1000 m, 975 s, 759 m, 736 m, 693 m, 527 s, 493 m. UV–visible and ^{31}P NMR spectroscopic data are given in Table I.

Preparation of $Ph_2PS_2N_3H^+CF_3SO_3^-$. A solution of CF_3SO_3H (0.68 g, 4.5 mmol) in 5 mL of CH_2Cl_2 was added dropwise to a stirred solution of $Ph_2PS_2N_3$ (0.56 g, 1.9 mmol) in 30 mL of CH_2Cl_2. The solvent was removed under vacuum to give a yellow oil, which was stirred rapidly with diethyl ether (20 mL) for 2 h. The resulting flocculent yellow precipitate was filtered off, dried under vacuum, and identified as $Ph_2PS_2N_3H^+CF_3SO_3^-$ (0.78 g, 1.7 mmol), mp 94–96 °C. Anal. Calcd for $C_{13}H_{11}F_3N_3O_3PS_3$: C, 35.37; H, 2.51; N, 9.52. Found: C, 34.92; H, 2.45; N, 9.61. IR (cm^{-1}): 3058 w, 2889 br, m, 2636 m, 1441 s, 1352 m, 1295 vs, 1279 s, 1232 vs, 1217 vs, 1185 s, 1165 s, 1158 s, 1121 vs, 1109 vs, 1072 m, 1022 vs, 990 m, 761 s, 751 m, 734 s, 695 m, 686 m, 647 m, 634 vs, 605 m, 526 vs, 515 m, 496 s, 435 m. UV–visible and ^{31}P NMR spectroscopic data are given in Table I.

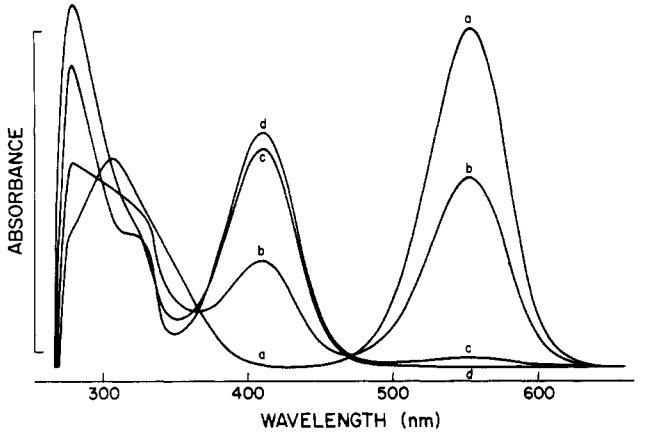

Figure 2. UV–visible spectra for the reaction of $HBF_4 \cdot Et_2O$ with $Ph_2PS_2N_3$ recorded at molar ratios of 0:1 (a), 0.5:1 (b), 1:1 (c), and 1.5:1 (d).

Table I. Visible Absorption and ^{31}P NMR Spectroscopic Data for Lewis Acid Adducts and Protonated and Methylated Derivatives of $Ph_2PS_2N_3$

adducts	λ_{max} (ϵ)[a,b]	$\delta(^{31}P)$[c]
$Ph_2PS_2N_3H^+BF_4^-$	410 (4.3×10^3)	7.9
$Ph_2PS_2N_3H^+CF_3SO_3^-$	410 (4.3×10^3)	7.7
$Ph_2PS_2N_3Me^+CF_3SO_3^-$	422 (2.9×10^3)	19.5
$Ph_2PS_2N_3 \cdot BCl_3$	427	16.8
$(Ph_2PS_2N_3)SnCl_4$	428	10.7
$Ph_2PS_2N_3$[d]	550 (5×10^3)	−21.2

[a] In CH_2Cl_2; λ_{max} in nm, ϵ in L mol^{-1}/cm^{-1}. [b] Accurate extinction coefficients could not be obtained for the BCl_3 and $SnCl_4$ adducts due to dissociation in solution. [c] Chemical shifts relative to 85% H_3PO_4 as external reference. [d] Data taken from ref 1.

Preparation of $Ph_2PS_2N_3Me^+CF_3SO_3^-$. An excess of $CF_3SO_3CH_3$ (0.58 g, 3.5 mmol) was added to a stirred solution of $Ph_2PS_2N_3$ (0.79 g, 2.7 mmol) in 30 mL of CH_2Cl_2, and the mixture was allowed to stir at room temperature for 2 days. The volume of the solution was reduced to 5 mL under vacuum and the residue was stirred rapidly with pentane (75 mL) for 1 day. The resulting yellow solid was removed by filtration and identified as $Ph_2PS_2N_3Me^+CF_3SO_3^-$ (1.20 g, 2.6 mmol) by X-ray crystallography. Anal. Calcd for $C_{14}H_{13}F_3N_3O_3PS_3$: C, 36.92; H, 2.88; N, 9.23. Found: C, 36.93; H, 3.17; N, 9.00. ^{13}C NMR (in $CDCl_3$): δ 44.4 (CH_3, d, $^2J_{PC}$ = 3.4 Hz). ^1H NMR (in $CDCl_3$): 3.31 (3 H, d, $^3J_{PH}$ = 11.0 Hz). IR (cm^{-1}): 3289 m, 3216 m, 1441 s, 1277 vs, 1256 vs, 1224 s, 1160 vs, 1117 vs, 1095 s, 1029 vs, 995 m, 981 m, 756 s, 735 s, 705 m, 692 m, 637 vs, 616 m, 602 m, 528 s, 516 s, 491 m. UV–visible and ^{31}P NMR spectroscopic data are given in Table I.

Preparation of $Ph_2PS_2N_3 \cdot BCl_3$. An excess of BCl_3 (1.0 M in hexanes, 2.6 mmol) was added by syringe to a stirred solution of $Ph_2PS_2N_3$ (0.64 g, 2.2 mmol) in 50 mL of diethyl ether. This mixture was allowed to stir at 23 °C to give a pale orange, microcrystalline product identified as $Ph_2PS_2N_3 \cdot BCl_3$ (0.74 g, 1.8 mmol), mp 106 °C dec. Anal. Calcd for $C_{12}H_{10}BCl_3N_3PS_2$: C, 35.28; H, 2.47; N, 10.29; S, 15.70; Cl, 26.04. Found: C, 35.40; H, 2.71; N, 10.32; S, 15.53; Cl, 25.86. IR (cm^{-1}): 1438 vs, 1119 vs, 1087 vs, 955 s, 938 vs, 833 m, 821 vs, 765 m, 753 s, 747 vs, 737 m, 730 m, 713 m, 703 m, 688 vs, 668 s, 646 m, 618 m, 609 m, 525 s, 498 vs. UV–visible and ^{31}P NMR spectroscopic data are given in Table I.

Preparation of $Ph_2PS_2N_3 \cdot SnCl_4$. An excess of $SnCl_4$ (1.0 M solution in CH_2Cl_2, 3.3 mmol) was added to a stirred solution of $Ph_2PS_2N_3$ (0.57 g; 2.0 mmol) in 30 mL of CH_2Cl_2. The solvent was removed under vacuum, and the light orange solid residue was stirred with *n*-pentane (40 mL) for 16 h. The product was separated by filtration and identified as the mono adduct $(Ph_2PS_2N_3)SnCl_4$ (0.97 g, 1.8 mmol), mp 104 °C dec. Anal. Calcd for $C_{12}H_{10}Cl_4N_3PS_2Sn$: C, 26.12; H, 1.83; N, 7.61. Found: C, 25.40; H, 1.80; N, 7.13. IR (cm^{-1}): 1438 s, 1120 vs, 1024 m, 996 m, 964 m, 896 m, 802 m, 745 m, 732 m, 687 s, 668 m, 648 m, 521 s, 497 m. UV–visible and ^{31}P NMR spectroscopic data are given in Table I. The product was recrystallized from carbon tetrachloride to give orange

Table II. Crystallographic Parameters

	trans-$(Ph_2PS_2N_3)_2SnCl_4$·2CCl_4	$Ph_2PS_2N_3Me^+CF_3SO_3^-$
formula	$C_{24}H_{20}Cl_4N_6P_2S_4Sn$·2$CCl_4$	$C_{14}H_{13}F_3N_3O_3PS_3$
fw	1009.01	440.04
space group	$P2_1/n$	$P2_1/a$
a, Å	9.238 (1)	11.857 (3)
b, Å	10.586 (1)	13.708 (2)
c, Å	21.752 (4)	12.417 (3)
β, deg	95.320 (8)	111.41 (1)
vol, Å^3	2118.1 (5)	1879.0 (7)
Z	2	4
D_{calcd}, g cm^{-3}	1.582	1.557
radiation, Å	Mo Kα (λ = 0.71069 Å, graphite monochromator)	
temp, °C	23 (2)	23 (2)
F(000)	996	892
scan range, ($\Delta\omega$), deg	1.5(0.80 + 0.347 tan θ)	1.5(0.72 + 0.347 tan θ)
scan speed, deg min^{-1}	0.5–3.3	0.5–3.3
max θ, deg	27	20
octants collcd	$-h,-k,\pm l$	$-h,+k,\pm l$
no. of unique reflcns	4607	1750
no. of obsd reflcns ($>3\sigma$)	3669	1432
μ(Mo Kα), cm^{-1}	13.99	5.19
min/max abs cor	0.860/1.126	0.847/1.107
weighting formula	$[\sigma^2(F) + 0.00005F^2]^{-1}$	
no. of reflcns used in final cycle	3669	1432
no. of variables in final cycle	233	184
GOF	1.481	1.383
R, R_w[a]	0.037, 0.042	0.050, 0.054
max shift/error in final cycle	0.09	0.003

[a] $R = \sum(||F_o| - |F_c||)/\sum|F_o|$; $R_w = [\sum w(|F_o| - |F_c|)^2/\sum w|F_o|^2]^{1/2}$.

crystals identified as the bis adduct *trans*-$(Ph_2PS_2N_3)_2SnCl_4$ by X-ray crystallography (vide infra). The bis adduct can be prepared in a nonpolar solvent as described below.

Preparation of $(Ph_2PS_2N_3)_2SnCl_4$. An excess of $SnCl_4$ (1.0 M in CH_2Cl_2, 3.0 mmol) was added by syringe to a stirred solution of $Ph_2PS_2N_3$ (0.68 g, 2.3 mmol) in 60 mL of a 5:1 mixture of pentane/CH_2Cl_2. The addition of the $SnCl_4$ resulted in an immediate decolorization of the purple solution and the production of a dark orange precipitate identified as $(Ph_2PS_2N_3)_2SnCl_4$ (0.92 g, 1.1 mmol) by comparison of the IR spectrum with that of an authentic sample; mp 131–133 °C. IR (cm^{-1}): 1438 m, 1120 vs, 1093 vs, 998 m, 936 m, 900 m, 761 m, 749 m, 733 vs, 712 m, 697 m, 687 s, 668 m, 601 m, 524 vs, 496 m.

X-ray Analyses. Crystals of $Ph_2PS_2N_3Me^+CF_3SO_3^-$ (**5**) were obtained from CH_3CN–Et_2O solution and crystals of $(Ph_2PS_2N_3)_2SnCl_4$ (**6**) were grown from a CCl_4 solution. The crystal data and experimental conditions are summarized in Table II. Both crystals were sealed in a glass capillary under nitrogen. The crystal of **5** was a plate having the dimensions 0.5 × 0.5 × 0.2 mm while the crystal of **6** was a fragment cut from a large crystal and had dimensions of approximately 0.5 × 0.4 × 0.3 mm. Cell constants and orientation matrices were determined by least-squares refinement of the diffraction geometry for 25 accurately centered reflections (**5**, 10° < θ < 17°; **6**, 13° < θ < 21°). The space groups were determined unambiguously by the systematic absences (**5**: $h0l$, $h = 2n + 1$; $0k0$, $k = 2n + 1$. **6**: $h0l$, $h + l = 2n + 1$; $0k0$, $k = 2n + 1$). The data were collected on an Enraf-Nonius CAD4F automated diffractometer using the ω–2θ scan technique. In the case of **5**, the crystal became dislodged in the capillary after the data were collected to 20° and data collection was stopped. A suitable second crystal could not be found. The data were corrected for background, Lorentz, and polarization effects as well as crystal decay[10] (7% and 12% drop in intensity of three standard reflections for **5** and **6**, respectively). The data were corrected for absorption by using an empirical method (DIFABS)[11] in order to account for irregular crystal shape, grease, and the capillary. Details concerning data collection and reduction can be found in ref 12.

Table III. Positional Parameters (×10^4) and B_{eq} (Å^2 × 10) or B_{iso} (Å^2 × 10)[a] for the Non-H Atoms of $Ph_2PS_2N_3Me^+CF_3SO_3^-$ (**5**)

atom	x/a	y/b	z/c	B_{eq} or B_{iso}
P	2747 (2)	1966 (1)	8263 (1)	28.9 (9)
S(1)	1844 (2)	2972 (1)	9709 (2)	45 (1)
S(2)	4042 (2)	3573 (1)	9489 (2)	39 (1)
N(1)	2261 (4)	1859 (3)	9361 (4)	32 (3)
N(2[	3017 (5)	3699 (4)	9974 (4)	44 (3)
N(3)	3939 (4)	2690 (3)	8664 (4)	33 (3)
C(1)	3062 (7)	1324 (5)	10392 (6)	54 (4)
C(11)	3199 (5)	809 (4)	7933 (5)	29 (1)
C(12)	2454 (6)	−3 (5)	7859 (5)	37 (2)
C(13)	2801 (6)	−908 (5)	7544 (6)	43 (2)
C(14)	3845 (7)	−978 (5)	7321 (6)	48 (2)
C(15)	4572 (6)	−174 (5)	7382 (6)	41 (2)
C(16)	4244 (6)	725 (5)	7685 (5)	33 (1)
C(21)	1542 (5)	2465 (4)	7080 (5)	29 (1)
C(22)	1740 (6)	3324 (5)	6575 (5)	36 (2)
C(23)	818 (6)	3683 (5)	5608 (6)	43 (2)
C(24)	−279 (6)	3205 (5)	5160 (6)	45 (2)
C(25)	−478 (6)	2361 (5)	5673 (6)	44 (2)
C(26)	428 (6)	1972 (5)	6654 (5)	37 (1)
S(3)	3771 (2)	5816 (1)	7432 (3)	43 (1)
O(1)	4464 (5)	4968 (3)	7899 (4)	61 (3)
O(2)	2505 (5)	5716 (5)	7212 (5)	82 (4)
O(3)	4316 (7)	6688 (4)	7921 (6)	96 (4)
C(2)	3798 (8)	5851 (8)	5993 (8)	64 (6)
F(1)	3221 (4)	6638 (4)	5412 (4)	86 (3)
F(2)	3223 (7)	5091 (5)	5385 (5)	116 (5)
F(3)	4867 (5)	5848 (5)	5979 (5)	135 (5)

[a] Phenyl C atoms (C(11)–C(26)) were refined with isotropic thermal parameters.

Table IV. Positional Parameters (×10^4) and B_{eq} (Å^2 × 10) for the Non-H Atoms of $(Ph_2PS_2N_3)_2SnCl_4$·2CCl_4 (**6**·2CCl_4)

atom	x/a	y/b	z/c	B_{eq}
Sn	5000	5000	5000	22.1 (1)
Cl(1)	5601.1 (11)	3340.8 (9)	4303.5 (4)	35.3 (4)
Cl(2)	6101.5 (11)	6484.5 (9)	4362.7 (4)	35.2 (4)
P	2036.6 (11)	6403.0 (9)	4051.5 (4)	27.9 (4)
S(1)	2169.9 (12)	3783.4 (9)	4192.9 (5)	35.0 (5)
S(2)	−533.5 (11)	5009.9 (12)	4201.1 (5)	42.1 (5)
N(1)	2876 (1)	5219 (2)	4426 (1)	27 (1)
N(2)	423 (4)	3788 (3)	4252 (2)	41 (2)
N(3)	268 (3)	6258 (3)	4084 (3)	37 (2)
C(11)	2448 (4)	7922 (4)	4373 (2)	32 (2)
C(12)	3449 (5)	8702 (4)	4133 (2)	41 (2)
C(13)	3679 (6)	9904 (5)	4370 (3)	57 (3)
C(14)	2912 (8)	10317 (5)	4848 (3)	67 (4)
C(15)	1906 (7)	9547 (6)	5092 (3)	62 (3)
C(16)	1677 (5)	8345 (4)	4854 (2)	47 (2)
C(21)	2381 (4)	6415 (3)	3253 (2)	30 (2)
C(22)	1499 (5)	7140 (4)	2841 (2)	43 (2)
C(23)	1720 (5)	7144 (5)	2223 (2)	49 (2)
C(24)	2778 (6)	6411 (4)	2014 (2)	45 (2)
C(25)	3666 (5)	5700 (5)	2416 (2)	47 (2)
C(25)	3467 (5)	5701 (4)	3041 (2)	39 (2)
C(1)	6967 (5)	9351 (5)	2763 (2)	53 (3)
Cl(3)	7895 (2)	9253 (2)	2090.8 (6)	75 (1)
Cl(4)	7777 (2)	8302 (2)	3307.6 (7)	84 (1)
Cl(5)	5148 (2)	8931 (2)	2558.0 (9)	89 (1)
Cl(6)	7073 (2)	10851 (2)	3063.1 (10)	96 (1)

[a] Phenyl C atoms (C(11)–C(26)) were refined with isotropic thermal parameters. [b] Sn is placed at the crystallographically imposed cetre of symmetry.

Atomic scattering factors for non-H atoms were those of Cromer and Mann,[13] the H scattering factors were taken from ref 14, and real and anomalous dispersion corrections were applied to all non-H atoms.[15] The

(10) All computations were performed with XRAY 76 unless otherwise stated; "XRAY 76"; Tecnnical Report TR-446; Stewart, J. M., Ed.; Computer Science Center, University of Maryland: College Park, MD, 1976.
(11) Walker, N.; Stuart, D. *Acta Crystallogr., Sect. A: Found. Crystallogr.* **1983**, *A39*, 158.
(12) Chivers, T.; Richardson, J. F.; Smith, N. R. M. *Inorg. Chem.* **1985**, *24*, 2453.
(13) Cromer, D. T.; Mann, J. B. *Acta Crystallogr., Sect. A: Cryst. Phys., Diffr., Theor. Gen. Crystallogr.* **1968**, *A24*, 321.
(14) Stewart, R. F.; Davidson, E.; Simpson, W. J. *Chem. Phys.* **1968**, *42*, 3175.
(15) *International Tables for X-ray Crystallography*; Kynoch: Birmingham, England, 1974.

structure of **5** was solved by using MULTAN 78,[16] which revealed the positions of the P, S, and N atoms. All remaining atoms were located by using difference Fourier and least-squares techniques. H atoms were included in the positions located on a difference Fourier map and given an isotropic thermal parameter of $1.1U_{iso}$ of the connected C atoms, but not refined. In the final cycle, the phenyl C atoms were refined isotropically and all other non-H atoms were refined with anisotropic thermal parameters. An isotropic extinction parameter could not be refined. Refinement was carried out by full-matrix least-squares techniques based on F, minimizing the function $\sum w(|F_o| - |F_c|)^2$. The structure of **6** was solved by placing the Sn atom on the crystallographically imposed center of symmetry ($^1/_2$, $^1/_2$, $^1/_2$) followed by a series of difference Fourier syntheses and least-squares cycles. H atoms were included in calculated positions and given a temperature factor of $1.1B_{eq}$ of the connected C atoms, but not refined. All non-H atoms were refined with anisotropic thermal parameters, and an isotropic extinction coefficient was refined to a value of 6.7 (1.1) $\times 10^{-4}$. In each case the residual electron density was small and not of chemical significance (**5**, 0.4 e Å^{-3} associated with C(24)–C(25); **6**, 1.03 e Å^{-3} associated with CCl_4 solvate). The final atomic coordinates of the non-H atoms of **5** and **6** are given in Tables III and IV, respectively.

Theoretical Method. All calculations were carried out by utilizing the HFS–LCAO program system developed by Baerends et al.[17] The *n*s and *n*p shells on N, P and S were represented by a double-ζ STO basis set augmented by a 3d STO for P and S (ζ^P_{3d} = 1.35, ζ^S_{3d} = 1.55). The 1s shell of the H atoms was represented by a double-ζ STO basis set, augmented by a single 2p STO (ζ^H_{2p} = 1.0)[18] in the case of the proton bonded to the N atom. The electrons in shells of lower energy on N, P, and S were considered as core electrons and were treated by the frozen-core approximation according to the procedure of Baerends et al.[17] The decomposition of the protonation energies into electronic and electrostatic components was accomplished according to the scheme of Rauk and Ziegler.[19]

Results and Discussion

Spectroscopic Investigation of the Reaction of HBF_4·Et_2O with $Ph_2PS_2N_3$ (1) (R = Ph). It was evident from our first efforts to prepare Lewis acid adducts of **1** that the endocyclic nitrogen atoms are only weakly basic since attempts to recrystallize the products from solvent mixtures containing diethyl ether regenerated **1**. In order to gain a more detailed understanding of adduct formation, the reaction of **1** with HBF_4 was monitored by ^{31}P NMR and by UV–visible spectroscopy over a range of HBF_4:$Ph_2PS_2N_3$ molar ratios. The ^{31}P NMR spectra for molar ratios of 0:1, 0.5:1, 1:1, and 1.5:1 are shown in Figure 1. These spectra clearly indicate that a rapid exchange process exists between the protonated and nonprotonated rings. This exchange process is manifested by a single time-averaged signal rather than the appearance of a new signal for the protonated ring and a decrease in the intensity of the signal attributed to **1** (R = Ph). Furthermore, the value of the ^{31}P NMR chemical shift of the reaction mixture does not change significantly when the molar ratio HBF_4:$Ph_2PS_2N_3$ exceeds 1:1 indicating that only monoprotonation occurs.

The UV–visible spectra for the HBF_4–$Ph_2PS_2N_3$ reaction at molar ratios of 0:1, 0.5:1, 1:1, and 1.5:1 are depicted in Figure 2. Addition of HBF_4 to a solution of **1** (R = Ph) in CH_2Cl_2 results in a decrease in the intensity of the absorption band at 550 nm due to **1** (R = Ph) and the appearance of a new absorption band at 410 nm attributed to the monoprotonated form of **1** (R = Ph). Isobestic points are observed at ca. 365 and 470 nm, indicating that $Ph_2PS_2N_3H^+$ and $Ph_2PS_2N_3$ are the only species present in appreciable concentrations in this system. At a 1:1 molar ratio the color of the solution has changed from purple to yellow; protonation is complete, and only dilution effects are observed upon further addition of HBF_4·Et_2O.

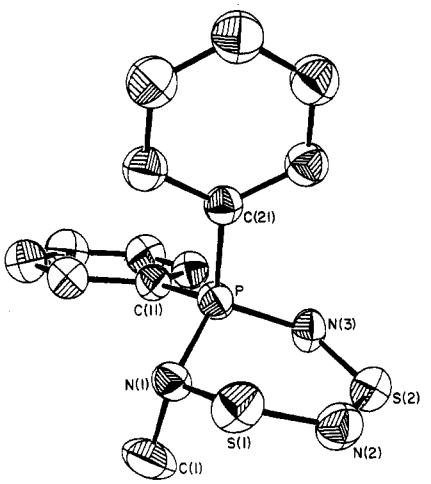

Figure 3. ORTEP plot (50% probability ellipsoids) of the $Ph_2PS_2N_3Me^+$ cation in **5**.

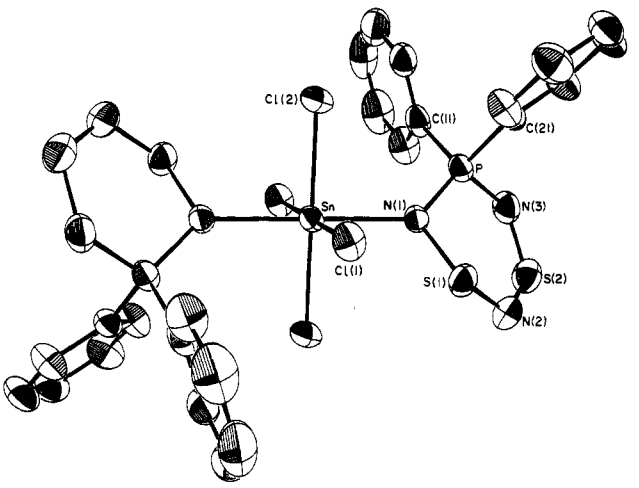

Figure 4. ORTEP plot (50% probability ellipsoids) of *trans*-$(Ph_2PS_2N_3)_2SnCl_4$.

Preparation and Spectroscopic Characterization of Lewis Acid Adducts and Protonated or Methylated Derivatives of 1 (R = Ph). The Lewis acid adducts of **1** (R = Ph) with BCl_3 or $SnCl_4$ and protonated or methylated derivatives of **1** (R = Ph) were obtained by addition of an excess of the appropriate reagent to a stirred solution of **1** (R = Ph) in a suitable solvent. The adducts were obtained as moisture-sensitive, yellow-orange solids that could be recrystallized without dissociation in the presence of an excess of the Lewis acid. In the case of $SnCl_4$ either a mono or a bis adduct could be obtained depending on the solvent system. In a nonpolar solvent the bis adduct is formed as an orange precipitate, while in CH_2Cl_2 the mono adduct is obtained.

The yellow-orange color of the adducts (λ_{max} = 410–430 nm) is in marked contrast to the intense purple color of **1** (R = Ph) (Table I). An indication of the strength of the interaction between **1** (R = Ph) and various acceptors is given by the fact that the visible absorption band for the protonated species is observed at ca. 410 nm and no dissociation in solution to give free ligand is evident, whereas the corresponding band for the BCl_3 and $SnCl_4$ adducts occurs at ca. 430 nm and the presence of free ligand in solution is readily detected by the appearance of a characteristic band at 550 nm. This dissociation is particularly marked for $(Ph_2PS_2N_3)_2SnCl_4$. Although the dark orange color of the bis adduct is obviously different from the pale orange of the solid mono adduct, the visible absorption spectrum of the bis adduct in CH_2Cl_2 shows only bands for the mono adduct and **1** (R = Ph).

The ^{31}P NMR chemical shifts of the adducts appear in the range +7 to +19 ppm compared to the value of −21 ppm for **1** (R = Ph) (Table I). The observation of coupling between the

(16) MULTAN 78 is a system of programs for the automatic solution of crystal structures from X-ray diffraction data: Main, P.; Hull, S. E.; Lessinger, L.; Germain, G.; Declercq, J.-P.; Woolfson, M. M. "MULTAN 78"; University of York: York, England, 1978.
(17) Baerends, E. J.; Ellis, D. E.; Ros, P. *Chem. Phys.* **1973**, *2*, 41.
(18) (a) Vernooijs, P.; Snijders, J. G.; Baerends, E. J. "Slater type basis functions for the whole periodic system", internal report; The Free University of Amsterdam: Amsterdam, The Netherlands, 1981. (b) Snijders, G. J.; Baerends, E. J.; Vernooijs, P. *At. Data Nucl. Data Tables* **1982**, *26*, 483.
(19) Ziegler, T.; Rauk, A. *Inorg. Chem.* **1979**, *18*, 1558.

Table V. Selected Bond Lengths (Å) and Bond Angles (deg) for $Ph_2PS_2N_3$ (**1** (R = Ph)), $Ph_2PS_2N_3Me^+CF_3SO_3^-$ (**5**), and *trans*-$(Ph_2PS_2N_3)_2SnCl_4 \cdot 2CCl_4$ (**6**·$2CCl_4$)[a]

	1 (R = Ph)	5	6
P(1)–C(11)	1.792 (4)	1.770 (6)	1.780 (4)
P(1)–C(21)	1.788 (4)	1.771 (5)	1.796 (4)
P(1)–N(1)	1.625 (3)	1.668 (6)	1.648 (3)
P(1)–N(3)	1.621 (4)	1.649 (5)	1.649 (3)
N(1)–S(1)	1.575 (3)	1.707 (5)	1.712 (3)
S(1)–N(2)	1.583 (5)	1.644 (6)	1.631 (4)
N(2)–S(2)	1.580 (4)	1.549 (7)	1.548 (4)
S(2)–N(3)	1.560 (3)	1.562 (5)	1.564 (4)
N(1)–C(1) (Sn)		1.481 (8)	2.239 (3)
N(1)–P(1)–N(3)	115.9 (2)	108.7 (3)	109.3 (2)
N(1)–P(1)–C(11)	109.9 (2)	109.6 (3)	114.8 (2)
N(1)–P(1)–C(21)	107.3 (2)	107.3 (3)	111.5 (2)
N(3)–P(1)–C(11)	108.5 (2)	108.1 (3)	104.1 (2)
N(3)–P(1)–C(21)	107.9 (2)	111.2 (3)	107.9 (2)
C(11)–P(1)–C(21)	107.1 (2)	112.0 (3)	108.8 (2)
P(1)–N(1)–S(1)	120.3 (2)	110.3 (3)	112.4 (2)
P(1)–N(1)–C(1) (Sn)		116.5 (5)	134.6 (2)
S(1)–N(1)–C(1) (Sn)		112.2 (4)	111.3 (1)
N(1)–S(1)–N(2)	116.3 (2)	106.8 (3)	109.1 (2)
S(1)–N(2)–S(2)	124.6 (3)	125.5 (4)	123.6 (2)
N(2)S(2)–N(3)	116.9 (2)	117.2 (3)	116.2 (2)
P(1)–N(3)–S(2)	121.3 (2)	121.1 (1)	125.3 (2)

[a] The atomic numbering schemes for **5** and **6** are given in Figures 3 and 4, respectively.

methyl group and the phosphorus atom ($^2J_{CP}$ = 3.4, $^3J_{HP}$ = 11.0 Hz) in the ^{13}C and ^1H NMR spectra of $Ph_2PS_2N_3Me^+CF_3SO_3^-$ (**5**) indicated that the site of attack was a nitrogen atom (N_a) adjacent to the phosphorus atom in **1** (R = Ph) rather than the unique nitrogen atom, N_b. This conclusion was confirmed by the X-ray crystallographic analyses of **5** and **6** described below.

X-ray Crystal Structures of $Ph_2PS_2N_3Me^+CF_3SO_3^-$ (5) and $(Ph_2PS_2N_3)_2SnCl_4 \cdot 2CCl_4$ (6·$2CCl_4$). The crystal structure of **5** consists of noninteracting $Ph_2PS_2N_3Me^+$ and $CF_3SO_3^-$ ions while that of **6** involves discrete molecular units with no unusual intermolecular contacts. ORTEP drawings of **5** and **6** with the atomic numbering schemes are displayed in Figures 3 and 4, respectively, and the pertinent endocyclic and exocyclic bond lengths and bond angles are compared with the corresponding values for **1** (R = Ph) in Table V. The endocyclic bond lengths of the common bonds in the PS_2N_3 rings of **5** and **6** are identical within experimental error. Both adducts also exhibit similar trends in endocyclic bond angles, although there are small differences in the absolute values of individual bond angles. The S(1)–N(2)–S(2)–N(3)–P(1) segment of the ring is planar to within 0.034 and 0.028 Å in **5** and **6**, respectively, while the coordinated nitrogen atom, N(1), is displaced from this plane by 0.78 and 0.71 Å in **5** and **6**, respectively. In contrast, the NSNSN unit is essentially planar in **1** (R = Ph), and the phosphorus atom is tilted out of this plane by 0.28 Å.

Coordination of $SnCl_4$ or a methyl group to N(1) causes a significant perturbation in the S–N bond lengths in the ring compared to those found for **1** (R = Ph).[1] Thus the S(1)–N(1) bond distance is 1.71 Å in the adducts (cf. 1.77 Å for the S–N single bond in H_3N–SO_3)[20] compared to 1.575 (3) Å in **1** (R = Ph). The S(1)–N(2) bond lengths of 1.644 (6) and 1.631 (4) Å are also longer in the adducts than in **1** [R = Ph, *d*(S(1)–N(2)) = 1.588 (5) Å], whereas the bond lengths N(2)–S(2) and S(2)–N(3) are shortened slightly to values in the range 1.55–1.56 Å, suggesting a tendency toward the formation of a localized four-π-electron system of a sulfur diimide.[21] Somewhat surprisingly, both P–N bonds in **5** and **6** are essentially equal in length and only slightly longer than the P–N bonds in **1** (R = Ph) (mean P–N bond length in **5** and **6** is ca. 1.65 Å compared to 1.62 Å in **1**). Thus the effect of adduct formation on P–N bond lengths is significantly less than that found for cyclophosphazenes.[5,6] The large difference in the angle sums at N(1) of 339° for **5** and 358.3° for **6** is primarily due to the disparity between the exocyclic bond angles of 116.5° for C(1)–N(1)–P and 134.6° for Sn–N(1)–P. The high value of the latter bond angle is probably due to repulsive steric interactions between phenyl groups on phosphorus and Cl(2) atoms in **6**.

The structural parameters for the heterocyclic rings in the adducts **5** and **6** are reminiscent of those found for $S_3N_3O_2^-$, in which the nitrogen adjacent to the oxidized sulfur atom is displaced 0.80 Å from the best plane and the S–N bond lengths, two of about 1.55 Å and the other two in the range 1.62–1.64 Å, reflect a tendency to form a sulfur diimide in the NSNSN segment of the ring.[22]

The two rings in **6** occupy trans positions in an approximately octahedral arrangement of ligands around the tin atom with bond angles in the range 88–92°, cf. *trans*-$SnCl_4 \cdot 2S_4N_4$.[23] The Sn–Cl distances are 2.385 (1) and 2.418 (1) Å; the shorter bonds involve the Cl atoms in close proximity to phenyl groups (cf. *d*(Sn–Cl) = 2.442 (6) Å in *trans*-$SnCl_4 \cdot 2S_4N_4$).[23] The Sn–N distance of 2.239 (3) Å is significantly longer than the corresponding value of 2.14 (2) Å observed for *trans*-$SnCl_4 \cdot 2S_4N_4$.[23]

Regiospecificity of the Protonation of 1 (R = Ph). Previous ab initio molecular orbital calculations for the model ring system **1** (R = H) have indicated that the nitrogen atom, N_a, adjacent to phosphorus carries a larger negative charge than the unique nitrogen atom, N_b.[1] Consequently, the site of attack by an electrophile on **1** is expected to be an N_a atom if electrostatic effects are dominant in this interaction. The spectroscopic and crystallographic results described above demonstrate that the reaction of **1** (R = Ph) with a variety of electrophiles occurs exclusively at N_a. In order to assess the relative importance of electronic or electrostatic effects in determining the regiospecifity of these reactions, we have carried out an analysis of the interaction energies for the model systems $H_2PS_2N_3H^+$ in which the proton is attached to either N_b, **7**, or N_a, **8**, using ab initio HFS–SCF

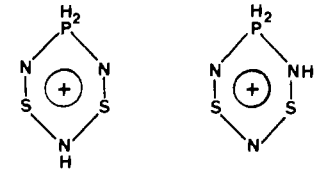

7 **8**

calculations. The calculations were carried out for N–H distances in the range 0.9–1.2 Å by using the experimental geometry of **1** (R = Ph) for the ring system.[1]

The electrostatic part represents, in our decomposition of the protonation energies, the electrostatic interaction energy between H^+ and the ring system of the protonated species, whereas the electronic part corresponds to the stabilization energy associated with charge rearrangements in the protonation process.

The trends in the electrostatic and electronic contributions to the interaction energies of **7** and **8** as a function of *d*(N–H) are shown in Figure 5. It is readily apparent from these data that the electronic energy contributions for **7** and **8** are essentially equal for all values of *d*(N–H) while the electrostatic interaction energy is significantly larger for **8** compared to that of **7**. For example, at *d*(N–H) = 1.0 Å this difference is ca. 13 kcal mol^{-1}. Thus it can be concluded that the site of attack on **1** by a proton is controlled by the electrostatic interaction. The observed preference for adduct formation at the nitrogen atom adjacent to phosphorus is consistent with the calculated atomic charge densities for **1** (R = H), which indicate that N_a carries a larger negative charge than N_b.[1]

(20) Cameron, A. F.; Duncanson, F. D. *Acta Crystallogr., Sect. B: Struct. Crystallogr. Cryst. Chem.* **1976**, *B32*, 1563.
(21) Typical S–N bond lengths in a *cis,cis*-sulfur diimide are ca. 1.52 Å. Gieren, A.; Betz, H.; Hübner, T.; Lamm, V.; Herberhold, M.; Guldner, K. *Z. Anorg. Allg. Chem.* **1984**, *513*, 160.
(22) Chivers, T.; Cordes, A. W.; Oakley, R. T.; Pennington, W. T. *Inorg. Chem.* **1983**, *22*, 2429.
(23) Martan, H.; Weiss, J. *Z. Anorg. Allg. Chem.* **1984**, *514*, 107.

Table VI. Orbital Overlap Populations

molecular orbital designation	ϵ, au	orbital overlap population								atom self-overlap population							
		PH(1)	PH(2)	PN(1)	PN(3)	N(1)S(1)	N(3)S(2)	S(1)N(2)	S(2)N(2)	H(1)	H(2)	P	N(1)	N(2)	N(3)	S(1)	S(2)
							(a) $H_2PS_2N_3$ (**1**(N))[a]										
1	−0.955	−0.002		0.003	0.006	0.009	0.058	0.028	0.079			0.01	0.03	0.20	0.13	0.04	0.20
2	−0.847	−0.001	0.001	−0.001	0.032	0.024	0.078	0.055	−0.006			0.02	0.04	0.13	0.25	0.14	0.08
3	−0.831	0.001	0.001	0.068	0.018	0.061	−0.009	−0.020	0.051			0.09	0.29	0.09	0.03	0.06	0.09
4	−0.674		−0.001	0.047	0.9014	−0.035	−0.019	0.067	0.024			0.04	0.15	0.10	0.10	0.31	0.20
5	−0.653	0.020	0.010	−0.014	0.047	0.038	0.034	−0.009	−0.016	0.01	0.01	0.34	0.05	0.09	0.08	0.09	0.18
6	−0.506	0.045	0.005	0.010	0.028	0.018	−0.004	0.018	0.005	0.03		0.26	0.05	0.06	0.14	0.08	0.19
7	−0.496	0.009	0.042	0.028	0.004	−0.012	−0.007	−0.018	−0.002	0.01	0.03	0.20	0.11	0.11	0.04	0.31	0.14
8	−0.447	0.036	0.033	0.006	0.028	0.008	0.010	0.007	0.017	0.04	0.03	0.22	0.02	0.05	0.10	0.08	0.10
9	−0.405		0.031	0.009	−0.002	0.002	0.003	0.031	0.055		0.03	0.09	0.04	0.19	0.06	0.15	0.20
10	−0.391	0.031	0.016	−0.004	0.010	−0.022	0.012	0.017	0.004	0.03	0.02	0.11	0.08	0.22	0.10	0.10	0.22
11[d]	−0.376	0.022	−0.001	−0.030	−0.010	0.013	0.019	−0.026	−0.004	0.02		0.20	0.17	0.07	0.13	0.23	0.22
12	−0.338	0.001	0.002	0.020	−0.019	0.023	−0.009	−0.022	−0.015			0.08	0.11	0.15	0.09	0.24	0.04
13[d]	−0.320	−0.001	0.001	0.014	−0.001	0.019	0.025	0.016	−0.022			0.04	0.11	0.06	0.30	0.34	0.10
14[d]	−0.278	0.004	0.025	−0.015	−0.009	0.002	0.028	0.012	0.004		0.05	0.07	0.27	0.23	0.26	0.03	0.04
15	−0.269	0.008	0.001	0.013	0.021	−0.005	−0.015	−0.008	−0.013	0.01		0.04	0.18	0.48	0.19	0.08	0.06
16	−0.238	0.001	0.008	0.017	0.002		−0.003	−0.007	0.005		0.02	0.06	0.46	0.07	0.19	0.10	0.10
17[d]	−0.197	−0.013	−0.002	0.019	0.017	−0.054	−0.039	−0.018	0.008	0.03		0.09	0.26	0.06	0.17	0.45	0.19
18[d,e]	−0.134	0.019	−0.031	−0.014	0.041	−0.029	−0.083	−0.053	−0.114		0.07	0.07	0.07	0.37	0.16	0.27	0.52
net π population[c]		0.048	0.092	−0.048	−0.012	−0.080	0.132	−0.064	−0.056	0.10	0.10	0.80	1.62	0.84	1.72	2.10	1.10
net population[c]		0.644	0.688	0.760	0.744	0.356	0.648	0.492	0.624	0.36	0.38	3.92	4.84	4.72	4.72	5.66	5.42
charge densities										0.32	0.29	−0.09	−0.34	−0.17	−0.28	0.12	0.14
							(b) $H_2PS_2N_3$ (**1**(P))[b]										
1	−0.960			0.008	0.008	0.031	0.036	0.047	0.050			0.01	0.08	0.19	0.09	0.09	0.11
2	−0.872			0.027	0.007	0.084	0.065	−0.004	0.010			0.01	0.20	0.01	0.13	0.16	0.16
3	−0.849	0.001	0.002	0.037	0.050	−0.001	0.016	0.048	0.027			0.10	0.09	0.23	0.16	0.04	0.03
4	−0.681			0.042	0.029	−0.030	−0.024	0.043	0.048			0.06	0.10	0.09	0.12	0.29	0.24
5	−0.671	0.012	0.020	0.006	0.026	0.045	0.015	−0.003	−0.014	0.01	0.01	0.34	0.06	0.09	0.06	0.12	0.16
6	−0.530			0.040	0.043	0.023	0.023	0.024	0.021			0.15	0.11	0.10	0.11	0.15	0.16
7	−0.495	0.048	0.046	0.009	0.009	−0.013	−0.014	−0.015	−0.014	0.03	0.03	0.34	0.06	0.03	0.06	0.19	0.18
8	−0.453	0.040	0.043	0.022	0.023	0.011	0.009	0.010	0.010	0.05	0.06	0.24	0.05	0.04	0.06	0.05	0.05
9	−0.404	0.025		0.004	0.014	−0.015	−0.001	0.036	0.033	0.02		0.08	0.08	0.21	0.09	0.15	0.15
10[d]	−0.396	0.014	0.043	0.003	0.003	−0.003	−0.001	0.036	0.027	0.01	0.04	0.15	0.04	0.22	0.04	0.12	0.13
11	−0.359	0.001	0.006	−0.025	−0.030	−0.013	−0.016	−0.050	−0.053		0.01	0.20	0.20	0.19	0.19	0.27	0.30
12[d]	−0.347			0.009	0.011	0.040	0.046	−0.004	−0.005			0.02	0.14	0.02	0.14	0.29	0.26
13	−0.340			0.011	0.011	0.030	0.034	−0.003	−0.005			0.02	0.13	0.02	0.13	0.32	0.29
14	−0.281	0.018	0.001	0.010	0.020	0.005	0.005	−0.007	−0.007	0.03		0.04	0.16	0.45	0.17	0.04	0.04
15[d]	−0.272	0.008	0.021	0.008	0.011	0.011	0.009	−0.012	−0.019	0.03	0.04	0.04	0.18	0.37	0.19	0.04	0.04
16	−0.260			−0.025	−0.025	−0.015	−0.012					0.07	0.37	0.08	0.35	0.14	0.14
17[d]	−0.185			0.029	0.030	−0.063	−0.065	0.001	−0.001			0.05	0.22		0.23	0.36	0.37
18[d,e]	−0.119	−0.064	0.005	0.033	0.032	−0.050	−0.046	−0.094	−0.093	0.14	0.03	0.14	0.07	0.38	0.06	0.43	0.41
net π population		0.088	0.256	0.196	0.220	−0.060	−0.044	0.084	0.008	0.08	0.16	0.52	1.16	1.22	1.20	1.62	1.60
net population		0.668	0.728	0.860	0.960	0.508	0.500	0.588	0.432	0.36	0.38	3.84	4.54	4.68	4.64	5.64	5.62
charge densities										0.33	0.31	−0.18	−0.19	−0.16	−0.26	0.08	0.08

[a] The designation **1**(N) refers to the ring geometry found for **5**, i.e. with the nitrogen atom out of the plane. [b] The designation **1**(P) refers to the ring geometry found for **1**(R = Ph) i.e. with the phosphorus atom out of the plane. [c] The net orbital overlap populations are given by 4 times the orbital sum where the factor of 4 arises due to doubly occupied orbitals giving a factor of 2 and the quadratic form of the population giving rise to another factor of 2. The net atom self-overlap populations indicate partial atomic population and, since all orbitals are doubly occupied, is 2 times the orbital sum. [d] π-Orbitals. [e] LUMO.

Table VII. Partitioned Occupations for $H_2PS_2N_3$: **1**(N) and **1**(P)[a]

	σ			π			
atom	s	p	d	s	p	d	total
H(1)	0.546 (0.556)			0.137 (0.120)			0.683 (0.676)
H(2)	0.588 (0.446)			0.118 (0.247)			0.706 (0.693)
P	1.364 (1.355)	2.306 (2.472)	0.604 (0.513)	0.022 (0.005)	0.435 (0.305)	0.325 (0.520)	5.076 (5.170)
N(1)	1.502 (1.573)	2.074 (2.449)		0.170 (0.068)	1.533 (1.170)		5.279 (5.260)
N(2)	1.523 (1.559)	2.282 (2.462)		0.272 (0.060)	1.260 (1.111)		5.337 (5.192)
N(3)	1.646 (1.578)	2.826 (2.282)		0.053 (0.132)	0.643 (1.165)		5.168 (5.157)
S(1)	1.701 (1.781)	2.620 (2.161)	0.430 (0.434)	0.099 (0.039)	0.756 (1.314)	0.238 (0.183)	5.844 (5.911)
S(2)	1.680 (1.768)	1.954 (2.143)	0.324 (0.443)	0.173 (0.064)	1.613 (1.309)	0.131 (0.190)	5.875 (5.917)

[a] The values for **1**(P) are given in parentheses.

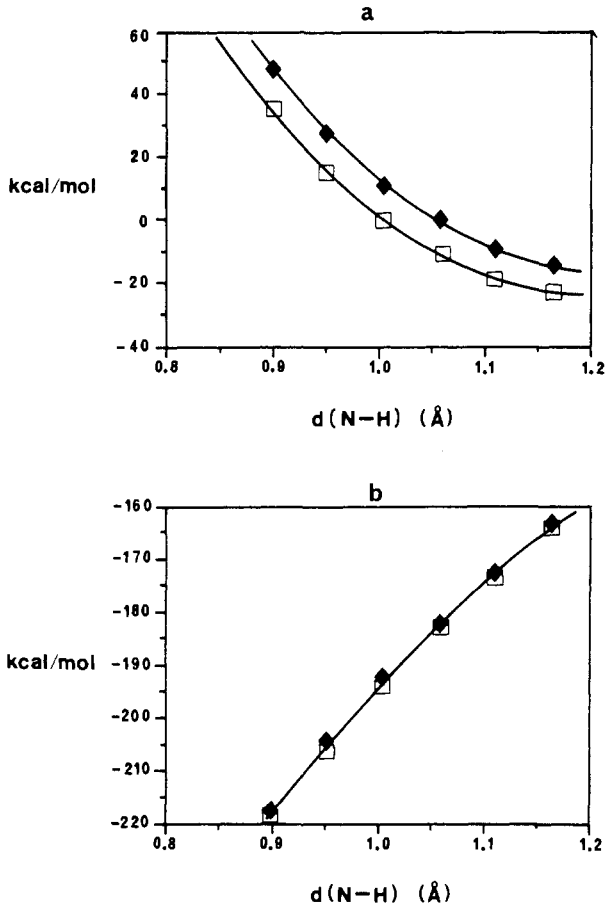

Figure 5. (a) Electrostatic interaction energy of **7** (◆) and **8** (□) as a function of d(N–H). (b) Electronic contribution to the interaction energy of **7** (◆) and **8** (□) as a function of d(N–H).

Geometry of the Protonated Ring in 8. There is a fundmental difference in the conformation of the heterocyclic ring in the adducts **5** and **6** compared to that in the present system **1** (R = Ph). In the former the nitrogen atom is tilted out of the plane of the other five atoms whereas in **1** (R = Ph) the S_2N_3 unit is planar and the phosphorus atom lies out of that plane. In order to understand the deformation of the ring in the adducts, we have calculated and compared the individual contributions to the interaction energy of the model protonated species $H_2PS_2N_3H^+$ (**8**) using the ring geometries found for (a) the methylated species **5** and (b) the original heterocyclic ring **1** (R = Ph) under C_1 symmetry with d(N–H) = 1.0 Å. These calculations show that the total interaction energy for **8** with the experimental geometry is ca. 17 kcal mol^{-1} greater than the corresponding value for the protonated form of the original ring structure. Analysis of the individual contributions to the total energy reveals that this stabilization is due entirely to electronic contributions; in fact, there is a destabilization of ca. 4 kcal mol^{-1} in the electrostatic contribution. However, the stabilization of 17 kcal mol^{-1} is partially offset by the destabilization effect of deforming the ring; the parent ring system with the out-of-plane nitrogen atom is less stable than the ring with phosphorus out of plane by ca. 7 kcal mol^{-1}. Thus the net effect is a stabilization of ca. 10 kcal mol^{-1} for the protonated species with the experimental geometry.

Electronic Structure of the Protonated Ring in 8. Many of the chemical and physical properties of π-electron-rich cyclophosphathiazenes can be explained from a knowledge of their electronic structures.[1] The hypsochromic shift observed in the visible spectra of the adducts of **1** (R = Ph) and the conformational changes found for the heterocyclic rings in **5** and **6** indicate that adduct formation has a marked influence on the electronic structure of the ring, especially with respect to the π-system.[24] This information does not, however, provide more than a superficial understanding of the changes that occur upon complexation. We have, therefore, undertaken a detailed analysis of the electronic structure of the model system $H_2PS_2N_3$ using the ring geometry found for **5**, i.e. with the *nitrogen atom out of the plane*, **1**(N). The results of this analysis, in the form of orbital overlap populations and partitioned occupations, are compared in Tables VI and VII, respectively, with similar data for $H_2PS_2N_3$ obtained by using the experimental ring geometry for **1** (R = Ph),[1] i.e. with the *phosphorus atom out of the plane*, **1**(P), under the same symmetry constraint (C_1).

The changes observed in the net (σ + π) orbital overlap populations in going from **1**(P) to **1**(N) do, as expected, reflect the changes in bond lengths and bond angles that occur upon adduct formation. Of more importance is the relationship between the changes in net overlap populations and changes in σ- and π-overlap populations. The data in Table VI show that deformation of the ring from **1**(P) to **1**(N) leads to a reduction in the total net overlap population from 5.24 to 4.96 indicating a lowering of the total bond order. Significantly, this decrease is due entirely to a net reduction in the π-overlap population from 0.75 to 0.01, which is partially offset by an increase in the σ-overlap population from 4.50 to 4.94. This reduction in effective overlap is also illustrated by the net atom self-overlap populations (Table VI). With the exception of S(2), which notably is part of the strengthened N(2)S(2)N(3) linkage, all atoms show increased total populations. Comparison of partitioned occupations for **1**(P) and **1**(N) reveals that all ring atoms except S(2) and N(2) show a net transfer of electrons from the σ- to the π-system. Thus the deformation of **1**(P) into **1**(N) results in a redistribution of π-electron density and an increase in the antibonding character of the π-system.

There are several additional features to note about orbital contributions to the σ- and π-systems. First, moving the phosphorus atom into the molecular plane reduces the participation of 3d orbitals in the π-system from 0.52 to 0.33 so that the phosphorus contribution to the delocalized π-orbitals is no longer dominated by the 3d contribution. Second, although the sulfur 3d contribution to the π-system remains small, the proportional contribution for S(2) is approximately doubled (from 0.18 out of 1.54 to 0.24 out of 1.09) due to a decreased p orbital contribution, and conversely, the 3d contribution for S(1) is reduced to a similar extent (from 0.19 out of 1.56 to 0.13 out of 1.92) due to an increased p orbital contribution to the π-system.

(24) The visible absorption band of **1** at ca. 550 nm has previously been assigned to the π*(HOMO) → π*(LUMO) transition.[1]

Calculations of the interaction of N(1) in **1**(N) and **1**(P) with a proton (vide supra) revealed that electron density is transferred to the proton primarily through orbitals 14 and 16 of **1**(P) and orbitals 14 and 17 (and, to a lesser extent, 15) for **1**(N). Since this interaction is expected to have a greater influence on bonds involving N(1), it should have a greater stabilizing effect on **1**(N) compared to **1**(P) [i.e. the net overlap population for P–N(1) and N(1)–S(1) is −0.025 for orbitals 14 and 16 of **1**(P) and −0.048 for orbitals 14 and 17 of **1**(N)]. Finally, we note that orbitals 14 and 17 for **1**(N) are π-orbitals. The net effect of this interaction would, therefore, appear to be a cancellation of the destabilizing effect on the π-system brought about by the change in ring geometry.

Electronic Spectra of Lewis Acid Adducts of 1 (R = Ph). All the adducts of **1** (R = Ph) exhibit an intense visible absorption band in the region 410–430 nm (Table I). The observed blue shift in the π^*(HOMO) → π^*(LUMO) transition of **1**[1] is consistent with the trend in the calculated energy difference E(LUMO) − E(HOMO) observed for the series **1**(P) → **1**(N) → $H_2PS_2N_3H^+$ (using the experimental geometry of **5**), viz. 0.066 → 0.063 → 0.075 au. The increase in the transition energy for $H_2PS_2N_3H^+$ is primarily due to stabilization of the HOMO.

Conclusion. The interaction of phosphadithiatriazines with Lewis/Brønsted acids occurs at a nitrogen atom adjacent to the phosphorus atom of the PS_2N_3 ring and is controlled by electrostatic effects. Coordination to an electrophile also imposes a marked perturbation on both the conformation of the ring and the S–N bond lengths. The S–N bond involving the coordinated nitrogen is weakened substantially, and this nitrogen atom moves out of the plane of the other ring atoms, indicating that it is removed from the π-system, which becomes localized in the SNSNP segment of the ring. These effects appear to parallel those found for $S_3N_3^-$.[7] However, in the case of $S_3N_3^-$, a more stable conformation is achieved through ring contraction to give **4** with an S–S bond and the coordinated nitrogen as an exocyclic substituent. For the PS_2N_3 ring this stabilization is attained by the movement of the coordinated nitrogen out of the plane of the other ring atoms rather than by ring contraction, which would involve the formation of an endocyclic P–S bond. The structural changes observed for the PS_2N_3 ring upon adduct formation suggest that electrophiles might be used to promote ring-opening reactions or polymerization via S(2)–N(2) bond cleavage. The formation of π-complexes (η^3, η^4, or η^5) between the adducts and suitable metal acceptors also appears worthy of investigation since coordination to nitrogen should minimize the occurrence of π to σ rearrangements.

Acknowledgment. We thank the NSERC (Canada) for financial support in the form of operating and infrastructure grants and a postgraduate scholarship to S.W.L. and Dr. K. A. Kerr for the use of the X-ray diffractometer.

Registry No. **1** (R = H), 112575-73-2; **1** (R = Ph), 76958-87-7; **6**, 112596-25-5; **8**, 112575-74-3; $Ph_2PS_2N_3H^+BF_4^-$, 112596-21-1; $Ph_2PS_2N_3H^+CF_3SO_3^-$, 112575-70-9; $Ph_2PS_2N_3Me^+CF_3SO_3^-$, 112575-72-1; $Ph_2PS_2N_3{\cdot}BCl_3$, 112596-22-2; $Ph_2PS_2N_3{\cdot}SnCl_4$, 112596-23-3.

Supplementary Material Available: Tables listing thermal parameters, the derived hydrogen positions, and all bond lengths and bond angles for **5** and **6** (7 pages); tables of calculated and observed structure factors for **5** and **6** (24 pages). Ordering information is given on any current masthead page.

Contribution No. 4466 from the Central Research and Development Department, E. I. du Pont de Nemours and Company, Inc., Wilmington, Delaware 19898

Sterically Hindered Magnesium Aryloxides

Joseph Calabrese, Martin A. Cushing, Jr., and Steven D. Ittel*

Received September 15, 1987

Reaction of $MgBu_2$ with sterically hindered phenols such as 2,6-di-*tert*-butyl-4-methylphenol (H-BHT) gives the dimeric bis(phenoxide), $(Mg(BHT)_2)_2$. Reactions with oxygen donors give the monomeric adducts $Mg(BHT)_2L_2$, where L = THF or methyl benzoate. Diethyl ether slowly gives an analogous bis adduct. The X-ray structure of the dimeric species $(Mg(BHB)_2)_2$ (bis(bis(2,6-di-*tert*-butylphenoxy)magnesium)) displays the steric crowding of the *tert*-butyl groups around the Mg_2O_2 core. Crystal data: monoclinic, $C2/c$, a = 44.629 (4) Å, b = 13.922 (2) Å, c = 20.067 (5) Å, β = 97.43° at −70 °C.

Introduction

The utility of dialkylmagnesium compounds in synthetic magnesium chemistry has been reported by several investigators.[1-4] Reactions with protic species evolve 2 equiv of the alkane to give the desired species in high yield. Our investigation of the factors that influence the behavior of high activity, high stereospecificity magnesium chloride supported catalysts for 1-olefin polymerization[5] led us to explore magnesium compounds with sterically hindered phenoxide ligands such as 2,6-di-*tert*-butyl-4-methylphenol. (In this paper, butylated hydroxytoluene will be referred to as H-BHT; BHT implies the deprotonated anion.) The chemistry developed here closely parallels chemistry reported for related zinc compounds[6] and is analogous to the chemistry reported for Grignard reagents with the same hindered phenols.[7,8]

Experimental Section

All manipulations were carried out in the nitrogen atmosphere of a Vacuum Atmospheres drybox. Solvents were dried by standard techniques.[9] Dibutylmagnesium in heptane from Alfa and "butylated hydroxytoluene" (H-BHT)(2,6-di-*tert*-butyl-4-methylphenol and "butylated hydroxy benzene" (H-BHB)(2,6-di-*tert*-butylphenol) from Aldrich were used as received. NMR spectra were recorded on NT Series GE spectrometers at 300 or 360 MHz proton frequencies. Chemical shifts (ppm) were referenced to residual protic solvent peaks or internal TMS. Spectra were recorded in standard pulsed FT mode at constant temperature, which was calibrated by using a precalibrated thermocouple. Elemental analyses were performed on all isolated compounds by Galbraith Laboratories, Knoxville, TN, and were satisfactory. Vapor pressure osmometry molecular weight determinations were also

(1) Goel, A. B.; Mehrotra, R. C. *Indian J. Chem., Sect. A* **1978**, *16A*, 428.
(2) (a) Duff, A. W.; Hitchcock, P. B.; Lappert, M. F.; Taylor, R. G.; Segal, J. A. *J. Organomet. Chem.* **1985**, *293*, 271. (b) Henderson, M.; Papasergio, R. I.; Raston, C. L.; White, A. H.; Lappert, M. F. *J. Chem. Soc., Chem. Commun.* **1986**, 672.
(3) Ashby, E. C.; Goel, A. B. *Inorg. Chem.* **1979**, *18*, 1306.
(4) Hey, E.; Engelhardt, L. M.; Raston, C. L. *Angew. Chem., Int. Ed. Engl.* **1987**, *26*, 81.
(5) (a) Ittel, S. D.; Mulhaupt, R.; Klabunde, U. *J. Polymn. Sci., Polym. Chem. Ed.* **1986**, *24*, 3447. (b) Ittel, S. D.; Mulhaupt, R.; Shreve, A. P.; Klabunde, U. In *Homogeneous and Heterogeneous Catalysis*; Yermakov, Y., Likholobov, V., Eds.; VNU Press: Utrecht, The Netherlands, 1986; p 431. (c) Shreve, A. P.; Mulhaupt, R.; Fultz, W.; Calabrese, J.; Robbins, W.; Ittel, S. D. *Organometallics*, in press. (d) Mulhaupt, R.; Klabunde, U.; Ittel, S. D. *J. Chem. Soc., Chem. Commun.* **1985**, 1745. (e) Klabunde, U.; Mulhaupt, R. U.S. Patent 4650778, 1987.
(6) Geerts, R. L.; Huffman, J. C.; Caulton, K. G. *Inorg. Chem.* **1986**, *25*, 1803.
(7) Coffield, T. H. U.S. Patent 2903487, 1959.
(8) Zass, E.; Isenring, H. P.; Etter, R.; Eschenmoser, A. *Helv. Chim. Acta*, **1980**, *63*, 1048.
(9) Shriver, D. F.; Drezdon, M. A. *The Manipulation of Air-sensitive Compounds*; Wiley: Chichester, England, 1986.

0020-1669/88/1327-0867$01.50/0